

## THERMODYNAMIC MODELING OF CARBON DIOXIDE SOLUBILITY IN AQUEOUS SOLUTIONS OF MONOETHANOLAMINE USING TWO PARAMETER EQUATIONS OF STATE BASED ON NON-RANDOM MIXING RULES

M. Koolivand-Salooki<sup>1\*</sup>, S. J. Poormohammadian<sup>2</sup>, P. Darvishi<sup>2</sup>, Asghar Lashanizadegan<sup>2</sup>

<sup>1</sup> Gas research division, Research Institute of Petroleum Industries, Tehran 14665-1998, Iran

<sup>2</sup> Chemical engineering department, Yasouj University, Yasouj, Iran

Received May 7, 2017; Accepted July 31, 2017

### Abstract

The solubility of carbon dioxide in monoethanolamine (MEA) solutions at low and high pressure ranges has been investigated with Peng-Robinson (PR) and Soave-Redlich-Kwong (SRK) equations of state (EOS). Random and non-Random mixing rules have been used to calculate the EOS parameters. Modeling results were compared with the experimental data in the literature for 15 and 30 mass percent of MEA. It was shown that the absolute average relative errors of thermodynamic modeling by random mixing rules at low pressure ranges are 18.3 and 23.8 percent for PR and SRK equations of state respectively. Also the results had more deviation from the experimental data by adding the binary interaction parameters ( $k_{ij}$ ) to the random mixing rules. Finally, the solubility of CO<sub>2</sub> is examined by non-random mixing rules and it was shown that the results of the thermodynamic modeling were in excellent agreement with the experimental data. The absolute average relative errors in this case were 1.7 and 3.6 percent for PR and SRK equations of states respectively. The results of this study were also compared with the other model results of e-NRTL, Extended UNIQUAC and a quasi-equilibrium model.

**Keywords:** CO<sub>2</sub> solubility; thermodynamic modeling; PR and SRK equations of state; Non-Random mixing rule; MEA-H<sub>2</sub>O-CO<sub>2</sub> system.

### 1. Introduction

Removal of the acid gases from industrial gas streams such as flue gas, synthesis gas and natural gas is very important to prevent global warming. The main part of these impurities is greenhouse gases such as carbon dioxide (CO<sub>2</sub>) and nitrous oxide and harmful hydrogen sulfide gas. CO<sub>2</sub> is the largest contributor in regards to its amount present in the atmosphere contributing to about 60% of the global warming effects [1]. Thus action should be taken to decrease the accumulation of CO<sub>2</sub> in the atmosphere. Among different developed methods in reduction of CO<sub>2</sub> emissions, the post combustion capture (PCC) of carbon dioxide and its storage technology is one of the solutions considered on a short-term schedule, as it does not require deep modifications of existing power stations [2-4]. The most mature technology for the CO<sub>2</sub> post-combustion is the amine-based absorption due to its high affinity to CO<sub>2</sub> [5-10]. CO<sub>2</sub> capture by alkanolamine solvents and stripping are considered the most feasible option for the removal of carbon dioxide because they provide high selectivity for acid-gas components over nonpolar species [11-14]. Monoethanolamine (MEA) is the proven solvent for this application. Currently used experimental techniques have failed to measure accurately VLE data for low acid gas partial pressures and loadings ( $\alpha$  = mole of CO<sub>2</sub> per mole of amine in the liquid phase). This has triggered a substantial research activity on VLE modeling that can accurately predict CO<sub>2</sub> solubility's in various amine solutions for different operating conditions [15]. Therefore, it is crucial to study the thermodynamic behavior of such non-ideal CO<sub>2</sub>-H<sub>2</sub>O-MEA system for better understanding of its vapor-liquid equilibrium (VLE) over wide ranges of operating conditions and thus better process design and simulation. Knowledge of the equili-

brium solubility of carbon dioxide in water solutions of MEA solution is essential in the design of natural gas and refinery gas absorption systems which remove carbon dioxide and thermodynamic of absorption remains the most important criteria for estimating the efficiency of absorbent for carbon dioxide capture. The efficiency of absorbent is mostly characterized from CO<sub>2</sub> absorption isotherms (VLE) where carbon dioxide equilibrium partial pressure (P<sub>CO<sub>2</sub></sub>) is computed as a function of solvent loading [16-18].

The thermodynamic models used to encounter with this problem can be grouped into three categories: 1-semi-emperical (simple) models. These are models that utilize simple mathematical relations for phase equilibria and fitted the constants of chemical equilibrium. Danckwerts *et al.* [19] were among the first to develop a thermodynamic model for aqueous CO<sub>2</sub>-alkanolamine systems. They used a pseudo-equilibrium constant for the absorption reaction with all activity coefficients equal to one but corrected approximately for the effects of ionic strength. The model presented by Kent and Eisenberg [20] was also one of the first widely used models. They assumed all activity and vapor-phase fugacity coefficients equal to one and represented the CO<sub>2</sub> and H<sub>2</sub>S partial pressures over aqueous solutions of MEA and diethanolamine (DEA) [21]. Rangwala *et al.* [22] measured the absorption rates of CO<sub>2</sub> into aqueous solutions of TEA, MDEA and blends of MEA with MDEA and TEA. They used a modified pseudo first order model based on the film theory and also assumed all the activity coefficients equal to one. 2-Excess Gibbs energy ( $\gamma-\phi$  approach) models. One example is the work of Deshmukh and Mather [23] who developed a model with activity and fugacity coefficients calculated on the basis of the Debye-Hückel theory and the Guggenheim equation. Fang-Yuan Jou *et.al.* [24] measured the solubility of CO<sub>2</sub> in 30 mass % of MEA solution and correlated the data by using the Deshmukh-Mather model. They assumed the Henry constants of CO<sub>2</sub> in the aqueous MEA solutions are equal to the Henry constants of CO<sub>2</sub> in water. A common feature for the previously mentioned models is that they all describe the VLE by utilizing Henry's law constants and different models to describe the liquid and the vapor phase. Regarding more sophisticated models the electrolyte NRTL model (e-NRTL) [25] and the extended UNIQUAC model of Thomsen and Rasmussen [26] stick out. The e-NRTL model has been applied to amine systems by several authors [27-31], whereas the extended UNIQUAC model has somewhat fewer applications [32-33]. 3- Equation of state ( $\phi-\phi$  approach) models. In the equations of state, most approaches are based on the electrolyte equation of state framework presented by Furst and Renon [34]. Huttenhuis *et. al.* [35] evaluated the solubility of H<sub>2</sub>S and CO<sub>2</sub> in aqueous solutions of MDEA and correlated the data with the electrolyte EOS model as originally proposed by Furst and Renon. Button and Gubbins [36] extended the SAFT theory to H<sub>2</sub>O-CO<sub>2</sub>-alkanolamine systems, but the predictability for CO<sub>2</sub> loaded systems are not evident based on the information given in the article. PR and SRK equations of state have been used widely in thermodynamic modelings. Zoghi *et. al.* [37] added the association contribution of Helmholtz free energy proposed by Wertheim to these equations and calculated the solubility of light reservoir gases in water. Recently, Ali *et al.* [10] studied the solubility of CO<sub>2</sub> in ionic liquid analogues called deep eutectic solvents (DESs) using Peng-Robinson EOS.

In the above mentioned models, many adjustable parameters have to be fitted with experimental data and describing both chemical and phase equilibrium simultaneously is very complex. Indeed, solving the complex nonlinear equations is computationally time-consuming. In this study, a simplified thermodynamic model is presented to devise the behavior of CO<sub>2</sub> absorption within aqueous solutions of MEA. Because EOS can be employed in high pressure conditions, like those found in industry [38], we used the PR and SRK equations of state with the aid of non-random mixing rules. Based on this procedure, the solubility of CO<sub>2</sub> can be calculated in the MEA-H<sub>2</sub>O-CO<sub>2</sub> system in wide ranges of pressure without adjusting many parameters or solving complex equations. The only parameter which is needed for the modeling is binary interaction coefficients ( $l_{ij}$ ) and ( $k_{ij}$ ) in nonrandom and random mixing rules respectively that should be adjusted with experimental data.

## 2. Theory

### 2.1. Thermodynamic models

Two parameters equations of state used in this study for determination the solubility of CO<sub>2</sub> are defined as follows [39].

#### 2.1.1 Peng- Robinson (PR) EOS

The PR equation of state is defined as follows [40]:

$$P = \frac{RT}{v-b} - \frac{a}{v(v+b)+b(v-b)} \quad (1)$$

where a and b are functions of the critical properties of the chemical species as follows:

$$a = 0.457235 \frac{(RT_C)^2}{P_C} [1 + m(1 - \sqrt{T_r})]^2 \quad (2)$$

and

$$b = 0.077796 \frac{RT_C}{P_C} \quad (3)$$

with

$$m = 0.37464 + 1.5422\omega - 0.26992\omega^2 \quad (4)$$

PR in terms of the compressibility factor Z takes the following form:

$$Z^3 - (1-B)Z^2 + (A - 2B - 3B^2)Z - (AB - B^2 - B^3) = 0 \quad (5)$$

where

$$A = \frac{aP}{(RT)^2} \quad (6)$$

$$B = \frac{bP}{RT} \quad (7)$$

#### 2.1.2 Soave-Redlich-Kwong (SRK) EOS

This equation is defined as follows [41]:

$$P = \frac{RT}{v-b} - \frac{a}{v(v+b)} \quad (8)$$

where

$$a = 0.42747 \frac{(RT_C)^2}{P_C} [1 + m(1 - \sqrt{T_r})]^2 \quad (9)$$

$$b = 0.08664 \frac{RT_C}{P_C} \quad (10)$$

with

$$m = 0.480 + 1.574\omega - 0.176\omega^2 \quad (11)$$

SRK in terms of the compressibility factor Z takes the following form:

$$Z^3 - Z^2 + (A - B - B^2)Z - AB = 0 \quad (12)$$

The definition of A and B is given in Eqs. (6) and (7) respectively.

The PR and SRK EOS defined above have been using for single component. SRK is more reliable for substances with small acentric factors, whereas PR gives reliable data for compounds with acentric factors around 1.3 [39]. These equations are applied to multicomponent systems by employing mixing rules to determine their parameters for mixtures. The parameters of EOS are considered to represent the attractive and repulsive forces between the molecules. Hence the mixing rules should describe the prevailing forces between molecules of different substances forming the mixture.

### 2.2. Random mixing rules

The attractive force between molecules i and j, represented by  $a_{ij}$  in EOS, which is of an energy nature, can be expressed in a simple geometric average form [42] as:

$$a_{ij} = (a_i a_j)^{1/2} \quad (13)$$

The repulsive force between molecules i and j, represented by  $b_{ij}$  in EOS, which has the characteristic of volume, can be determined by arithmetic average:

$$b_{ij} = (b_i + b_j)/2 \quad (14)$$

Thus

$$a = \sum_i \sum_j x_i x_j a_{ij} \quad (15)$$

$$b = \sum_i \sum_j x_i x_j b_{ij} = \sum_i \sum_j x_i x_j \left( \frac{b_i + b_j}{2} \right) = \sum_i x_i b_i \quad (16)$$

It is common to incorporate an additional parameter in Eq. (15) to express the attractive term between pairs of non-similar molecules:

$$a_{ij} = (a_i \cdot a_j)^{\frac{1}{2}} (1 - k_{ij}) \quad (17)$$

where  $k_{ij}$  is known as the binary interaction parameter (BIP).

BIP is generally determined by minimizing the difference between predicted and experimental data, mainly the saturation pressure, of binary systems. Thus a BIP should be considered as a fitting parameter and not a rigorous physical term. Hence, the interaction parameters developed for any EOS should generally be used only for that EOS. Typically, the  $k_{ij}$  is between 0.0 and 0.20 for nonpolar or weakly polar systems, and can be larger or even negative for polar ones. For hydrocarbons that are not very different in size, the zero value can be used. The values of BIPs for each system should be adjusted with experimental data and for some systems have been shown and reported in the literature. Danesh *et al.* [39] reported a big dataset for PR and SRK EOS.

There is no doubt that the inclusion of binary interaction parameters in EOS mixing rules will provide more flexibility, and in most cases reliability at least within a limited working range. It is particularly a powerful tool to calibrate EOS for a reservoir fluid against the available experimental data. Additional flexibility can also be obtained by making BIP temperature [43], pressure [44], and composition dependent [45]. It should be noted that making BIP dependent on pressure or composition causes additional complexity in the expression for fugacity calculation of each component. The flexibility achieved by inclusion of BIP, particularly variable ones, can be quite misleading, as excellent results can be obtained for binary systems. That, however, only demonstrates a successful curve-fitting. The results for multicomponent systems particularly within wide ranges of temperature and composition may be quite disappointing. A comparative study of ten EOS indicated that the Patel and Teja equation as modified by Danesh *et al.* [46], without any BIP was more successful in modeling of the phase behavior of reservoir hydrocarbon fluids than others with BIP. Also Nasrifar *et. al.* [47] used ten EOS and predicted the thermodynamic properties of natural gas mixtures with zero binary interaction parameters.

### 2.3. Non-Random Mixing Rules

The random mixing rules that discussed in the previous section are quite adequate to describe hydrocarbon mixtures of reservoir fluids [39]. However, they cannot represent the interactions between hydrocarbons and asymmetric compounds such as water, or methanol which is often added to reservoir fluids as a hydrates inhibitor [39]. Although additional flexibility that is achieved by increasing the number of coefficients in binary interaction parameters may provide acceptable results for binary mixtures containing these compounds, the model can fail completely for multicomponent systems [48].

The assumption of random mixing rules in systems containing highly polar and asymmetric compounds is not justified as the existence of particular forces between some molecules, such as those due to permanent dipoles, may result in non-uniform distribution at the molecular level. Local composition mixing rules address this behavior by relating the attractive term in EOS to composition with a higher order polynomial than quadratic. The majority of mixing rules for the above term can be represented by the following form,

$$a = a^C + a^A \quad (18)$$

Where the attractive term is separated into two parts,  $a^C$ , which is the conventional random mixing term given by Eq.(15), and  $a^A$ , which is the asymmetric term due to polarity.

Avlonitis *et al.* [49], proposed a mixing rule for mixtures as follows:

$$a^A = \sum_p x_p^2 \sum_i l_{pi} x_i (a_p a_i)^{1/2} \quad (19)$$

Here the subscript p refers to the index of polar components, and  $l_{pi}$  is the binary interaction coefficient with  $l_{ij} = -l_{ji}$ . To describe the phase equilibria accurately over a wide range of tem-

peratures for polar systems, the binary interaction coefficients depend on temperature. The binary interaction coefficients should be a decreasing function of temperature as the asymmetric non-ideality reduces with temperature and were expressed by [39]:

$$l_{pi} = l_{pi}^0 - l_{pi}^1(T - 273) \quad (20)$$

where  $l_{pi}^0$  and  $l_{pi}^1$  are constants that should be fitted with experimental data, and T is in K.

Avlonitis *et.al.* [49] and Mathias *et.al.* [50] have been calculated them for different pairs of components but for MEA-CO<sub>2</sub>-H<sub>2</sub>O system, they have not been represented anywhere yet. The above mixing rule is quite flexible, particularly with temperature dependent interaction coefficients, and capable of describing the behavior of multicomponent mixtures containing highly asymmetric components when used in a cubic EOS [39]. Although Non-random mixing rules are very applicable, but they have not been used much in simulations. Up to our knowledge only Rahim Masoudi *et. al.* [51] have applied them in the modeling of gas hydrate inhibition by salts and organic inhibitors.

The VLE is obtained using the homogeneous approach ( $\phi-\phi$  method) based on the calculated fugacity for each component in both the liquid and vapor phases using the PR or SRK cubic EOS as follows:

$$\hat{f}_i^L = \hat{f}_i^v \quad (21)$$

where

$$\hat{f}_i^L = x_i \phi_i^L P \quad \hat{f}_i^v = y_i \phi_i^v P \quad (22)$$

with

$$\ln \phi_i = \frac{b_i}{b} (Z - 1) - \ln(Z - B) - \frac{A}{B(\delta_2 - \delta_1)} ((2 \sum_{j=1}^N x_j a_{ij}) / a - \frac{b_i}{b} \ln(\frac{Z + \delta_2 B}{Z + \delta_1 B})) \quad (23)$$

Where,  $\delta_1$ , and,  $\delta_2$ , are constants equal to 1 and 0 in SRK, and  $1 + \sqrt{2}$ , and  $1 - \sqrt{2}$  in PR EOS, respectively.

## 2.4. Solution procedure

In this research the VLE calculations is an iterative procedure where the liquid and vapor mole fractions are determined at a fixed temperature and pressure. The steps required to calculate the solubility of CO<sub>2</sub> in the MEA-H<sub>2</sub>O-CO<sub>2</sub> system based on non-random mixing rules are as follows:

1. Find the required properties for each component from table 1 and calculate  $a$  and  $b$  for each species from Eqs. (2) and (3) for PR and Eq. (9) and (10) for SRK respectively.
2. The vapor phase in this case is approximately pure CO<sub>2</sub>. Thus take the mole fraction of the components such that we have very little amount of MEA and H<sub>2</sub>O ( $y_2$  and  $y_3$ ) and remember that  $\sum_i y_i = 1$ .
3. Find  $a$  in terms of binary interaction coefficient ( $l_{ij}$ ) using Eq. (18) and (19).
4. Calculate  $b$  for the vapor mixture using Eq. (16).
5. Find the other necessary parameters,  $A$  and  $B$  and  $\phi_i^v$  in terms of binary interaction coefficient using Eq. (6), (7) and (23) respectively.
6. To adjust the binary interaction coefficients, use the experimental data and find the mole fraction of each component in the liquid phase ( $x_1$ ,  $x_2$ ,  $x_3$ ).
7. Repeat steps 3 to 5 and find  $a$ ,  $b$ ,  $A$ ,  $B$ ,  $\phi_i^L$  in terms of binary interaction coefficient for liquid phase.
8. Use equation (21) for each component and solve the set of equations to find the binary interaction coefficient ( $l_{ij}$ ). In the data fitting all experimental values were considered, and the square root of the sum of the squares of relative deviations of predictions were minimized. The adjusted values for our system are represented in table 2 and 3 for PR and SRK-EOS respectively.
9. Repeat steps 1-5 and calculate the vapor phase parameters with the binary interaction coefficients that were obtained in step 8.
10. Assume the mole fractions in the liquid phase and remember that  $\sum_i x_i = 1$ .
11. Repeat steps 3-5 and calculate the liquid phase parameters with the binary interaction coefficient that obtained in step 8.

12. Use equation (21) for each component and solve the set of equations to find the mole fraction of each component in the liquid phase.

13. Compare the calculated  $x_i$  in step 12 with the assumed  $x_i$  in step 10. If the absolute difference is less than a tolerance value, then the assumed  $x_i$  is the solubility of component  $i$  in the liquid phase otherwise go to step 8 and estimate a new value for  $x_i$ . Figure 1 shows the flowchart of the modeling for CO<sub>2</sub> solubility based on non-random mixing rules.

Table 1. Properties of the components

	MW(g/mol)	T <sub>c</sub> (k)	P <sub>c</sub> (bar)	$\omega$ (acentric factor)
CO <sub>2</sub>	44.01	304.21	72.86	0.224
MEA	61.08	671.4	80.3	0.7966
H <sub>2</sub> O	18.01	647.3	221.2	0.344

Table 2. Binary interaction coefficient for PR-EOS in MEA-CO<sub>2</sub>-H<sub>2</sub>O system

	$l_{pi}^0 l_{pi}^1 E4$	$l_{ij} = l_{pi}^0 - l_{pi}^1(T - 273)$ eq.20	313 K	353 K	393 K
MEA-CO <sub>2</sub>	0.03	10.72	-0.0288	-0.05576	-0.09864
MEA-H <sub>2</sub> O	-0.068	1.74	-0.07496	-0.08192	-0.08888
H <sub>2</sub> O-CO <sub>2</sub>	0.7148	22.89	0.6249	0.53512	0.44525

Table 3. Binary interaction coefficient for SRK-EOS in MEA-CO<sub>2</sub>-H<sub>2</sub>O system

	$l_{pi}^0 l_{pi}^1 E4$	$l_{ij} = l_{pi}^0 - l_{pi}^1(T - 273)$ eq.20	313 K	353 K	393 K
MEA-CO <sub>2</sub>	0.015	-8.33	0.04832	0.08164	0.11496
MEA-H <sub>2</sub> O	-0.023	-2.81	-0.01176	-0.00052	0.01072
H <sub>2</sub> O-CO <sub>2</sub>	-0.5338	-17.44	-0.46404	-0.39428	-0.32452

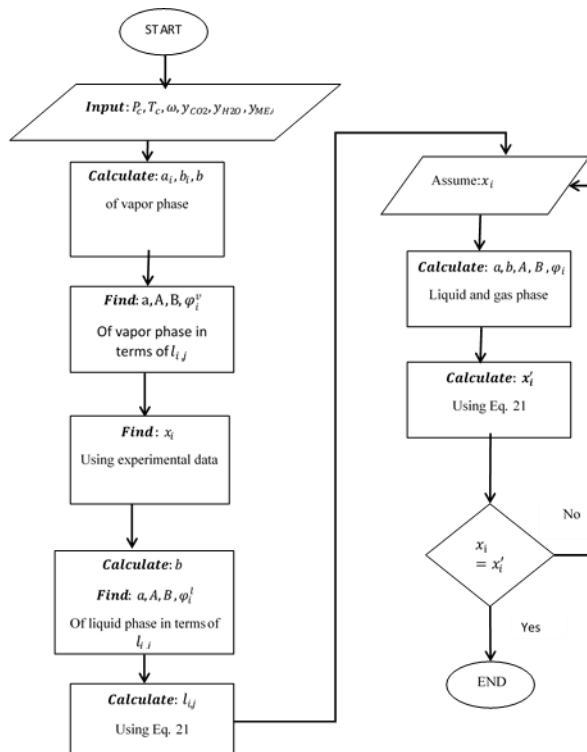


Figure 1. Modelling flowchart

Once the VLE is satisfied, the CO<sub>2</sub> solubility in the liquid phase is taken as its mole fraction in the liquid phase, i.e.,  $x_{CO_2}$ . The entire VLE calculation has been carried out in MATLAB software [52]. The solubility of CO<sub>2</sub> at different temperatures (313, 353 and 393) K in low and high pressure ranges calculated and compared with the experimental data reported by Wagner et.al. [3]. These experimental data were chosen because they are more reliable than other experimental data in the literature. Most methods used in literature [24,53-56] determined the CO<sub>2</sub>-concentration in the liquid phase by precipitation with BaCl<sub>2</sub> and subsequent titration and reveal also a large scattering. This method, however, has an estimated error of at least 3 % [24] and is thus less reliable than the gravimetric determination of the CO<sub>2</sub> concentration used by Wagner et.al. [3]. The total relative uncertainty of the amount of CO<sub>2</sub> in the liquid phase reported by Wagner et.al. [3] ranges from about ± 0.04 % at 313 K to

about  $\pm 0.6\%$  at 393K. indeed, most literature data reported for 393 K were determined at low gas loadings ( $\alpha < 0.5$ ), whereas the experimental results of Wagner et.al are for higher gas loadings ( $0.5 < \alpha < 0.7$ ).

### 3. Results and discussion

Most of the results available in the literature are given as partial pressure of CO<sub>2</sub> versus loading. The loading is given as

$$\alpha = \frac{\bar{m}_{CO_2}}{\bar{m}_{MEA}} \quad (24)$$

Where  $\bar{m}_{CO_2}$  and  $\bar{m}_{MEA}$  are molality (mol. (kg H<sub>2</sub>O)<sup>-1</sup>) of CO<sub>2</sub> and MEA respectively. In this study we also calculated  $\alpha$  and the absolute relative error (ARE) according to the following relationship:

$$Absolute\ Relative\ Error( ARE)\ \% = \frac{|\alpha_{(model)} - \alpha_{(experimental)}|}{\alpha_{(experimental)}} \times (100) \quad (25)$$

The errors have been calculated for each point and the absolute average relative error (AARE) for each model has been calculated by taking an average over all the points:

$$AARE = \frac{\sum ARE}{number\ of\ points} \quad (26)$$

#### 3.1. Prediction of solubility by random mixing rules

Figures 2 and 3 shows the solubility of CO<sub>2</sub> in the MEA-H<sub>2</sub>O-CO<sub>2</sub> system at high pressure ranges for 15 (2.9 mole MEA/kg H<sub>2</sub>O) and 30 (7 mole MEA/ kg H<sub>2</sub>O) mass percent of MEA respectively. The figures illustrate that PR equation of state overestimate and SRK equation of state underestimate the partial pressure of CO<sub>2</sub> for this system. As it can be seen from the figures, these predictions have deviations from the experimental data. In these cases the AAREs were 26.6 and 34.5 percent for PR and SRK EOS respectively. Another point is that in comparison of figures 2c and 3c with 2a and 3a mutually, the errors decrease to about 5 percent by increasing the temperature.

Figures 4 and 5 represent the solubility of CO<sub>2</sub> for the CO<sub>2</sub>-H<sub>2</sub>O-MEA system at low pressure ranges. The curves reveal that the errors are less than high pressure ranges. The AAREs were 18.3 and 23.8 percent for PR and SRK EOS accordingly. The effect of temperature is the same as in the high pressure ranges.

Another point that can be concluded from the figures 2 to 5 is that the solubility of CO<sub>2</sub> increases with increasing pressure and decreases with increasing temperature and it is due to the variations of density with pressure and temperature. The density of carbon dioxide in these ranges of pressure and temperature increases by adding system pressure and decreases with increasing system temperature. Thus there is a priori that the solubility of CO<sub>2</sub> is density dependent. At higher densities, the molecular interactions between the solvent (MEA solutions) and the solute (CO<sub>2</sub>) are enhanced and as a result, more solute is dissolved and this density effect on solubility enhancement at a higher density (higher pressure).

#### 3.2. Prediction of solubility by random mixing rules and inclusion of binary interaction parameters (BIP)

We used equation (17) to predict the solubility of CO<sub>2</sub> in this system. The deviations from experimental results were very high and the AAREs were more than 120 percent for PR EOS and more than 80 percent for SRK EOS in this case. As mentioned before the inclusion of BIP may provide acceptable results for binary mixtures but the model can fail completely for multicomponent systems [48]. The results for three cases have been sketched in figure 6.

#### 3.3. Prediction of solubility by non-random mixing rules

In order to compare random and non-random mixing rules we utilized equations (18) and (19) and took the solution procedure to find the mole fraction of carbon dioxide in the liquid phase. Figures 7 and 8 show the solubility of CO<sub>2</sub> versus its partial pressure in high pressure ranges (5-9 MPa) for 15 and 30 mass percent of MEA respectively. The AAREs were 2.3 percent for PR and 5.8 percent for SRK equation of state. Another important point that could be drawn from

the curves is that PR EOS works better in lower limit of this range (5-3 MPa) while SRK EOS has better performance in upper limit of this operating range (6-9 MPa). Both of the equations had approximately same deviation from experimental results in the middle part of the mentioned range (3-6 MPa) but PR overestimated and SRK underestimated the solubility.

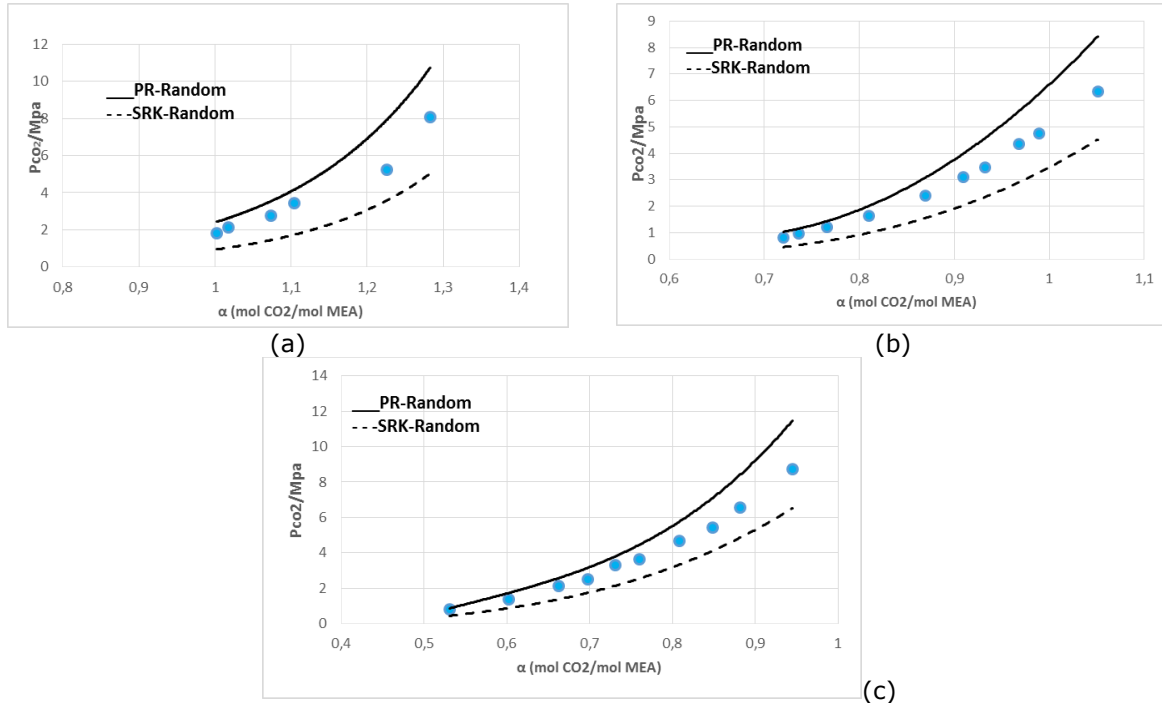


Figure 2. Solubility of  $\text{CO}_2$  in  $\text{CO}_2\text{-H}_2\text{O}\text{-MEA}$  system.  $m_{\text{MEA}} = 2.9 \text{ mol}\cdot(\text{kg H}_2\text{O})^{-1}$ . a)  $T=313 \text{ K}$ . b)  $T=353 \text{ K}$ . c)  $T=393 \text{ K}$ . ●, Experimental results of Wagner *et al.* [3]; Lines: model results

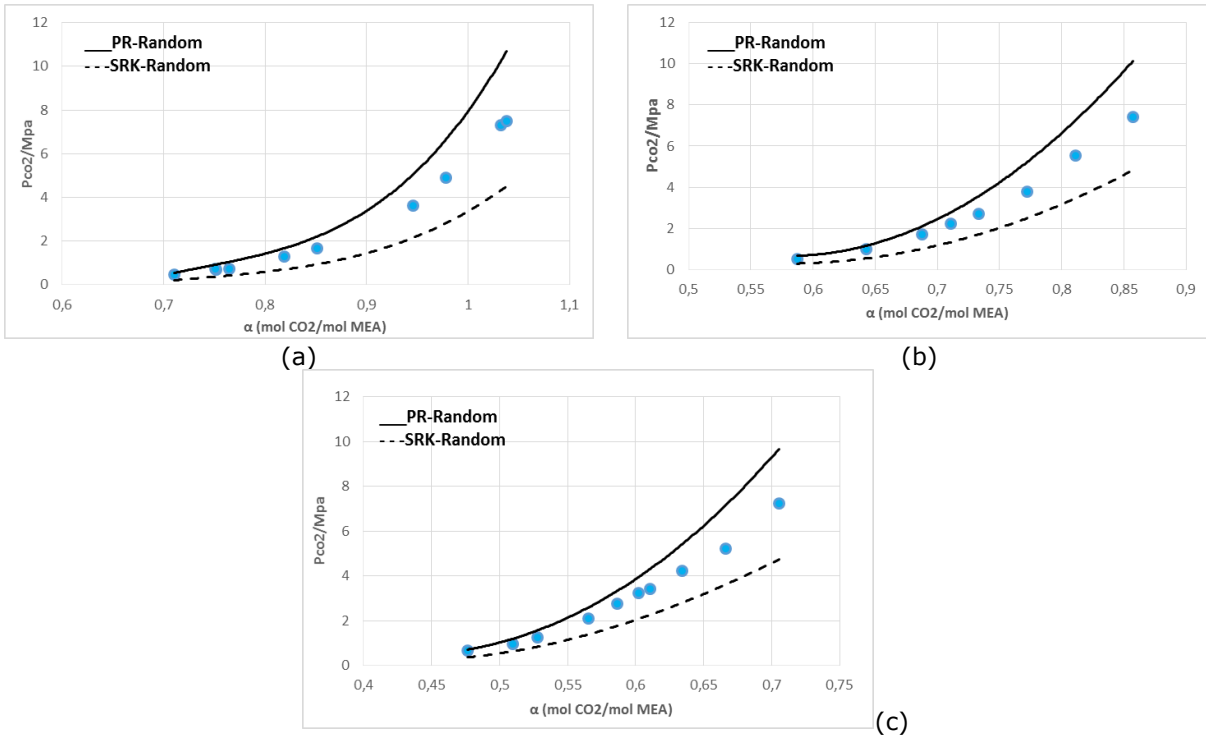


Figure 3. Solubility of  $\text{CO}_2$  in  $\text{CO}_2\text{-H}_2\text{O}\text{-MEA}$  system.  $m_{\text{MEA}} = 7.0 \text{ mol}\cdot(\text{kg H}_2\text{O})^{-1}$ . a)  $T=313 \text{ K}$  b)  $T=353 \text{ K}$ , c)  $T=393 \text{ K}$ . ●, Experimental results of Wagner *et al.* [3]; lines: model results

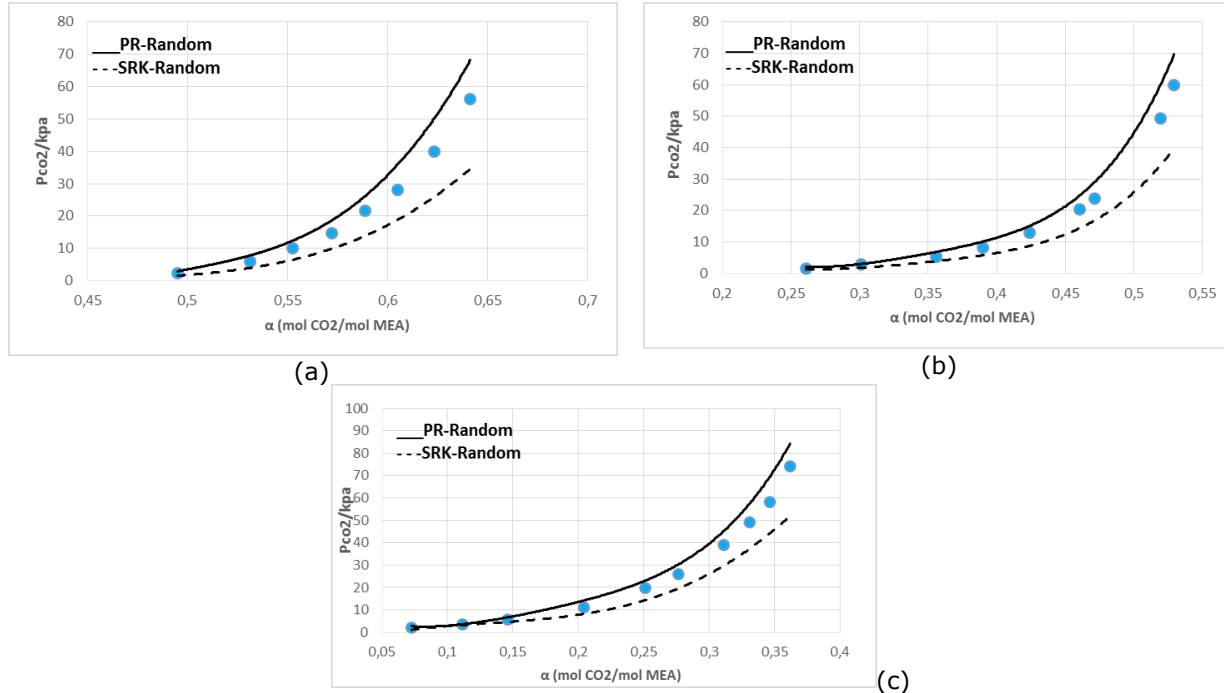


Figure 4. Solubility of CO<sub>2</sub> in CO<sub>2</sub>-H<sub>2</sub>O-MEA system.  $\bar{m}_{\text{MEA}} = 2.9 \text{ mol} \cdot (\text{kg H}_2\text{O})^{-1}$ . a) T=313 K. b) T=353 K. c) T=393 K. ●, Experimental results of Wagner *et al.* [3]; lines: model results

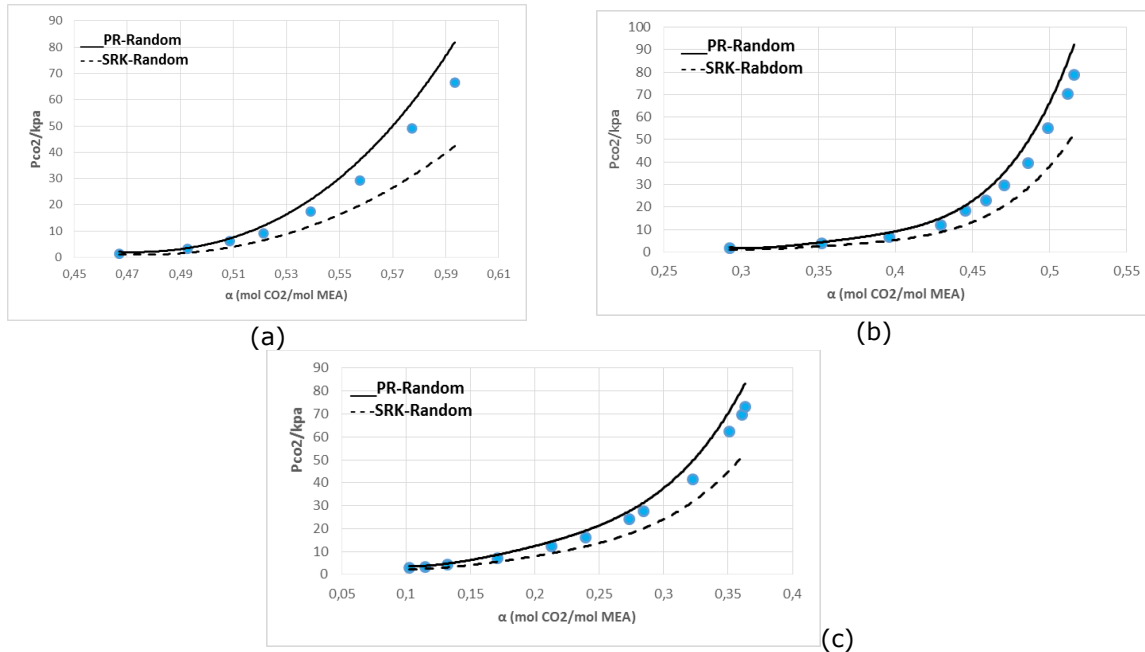


Figure 5. Solubility of CO<sub>2</sub> in CO<sub>2</sub>-H<sub>2</sub>O-MEA system.  $\bar{m}_{\text{MEA}} = 7.0 \text{ mol} \cdot (\text{kg H}_2\text{O})^{-1}$ . a) T=313 K. b) T=353 K. c) T=393 K. ●, Experimental results of Wagner *et al.* [3]; lines: model results

Table 4. Absolute average relative errors (AARE)

	High Pressure PR EOS	High Pressure SRK EOS	Low Pressure PR EOS	Low Pressure SRK EOS
Random Mixing Rules	26.6	34.5	18.3	23.8
Non-Random Mixing Rules	2.3	5.8	1.7	3.6

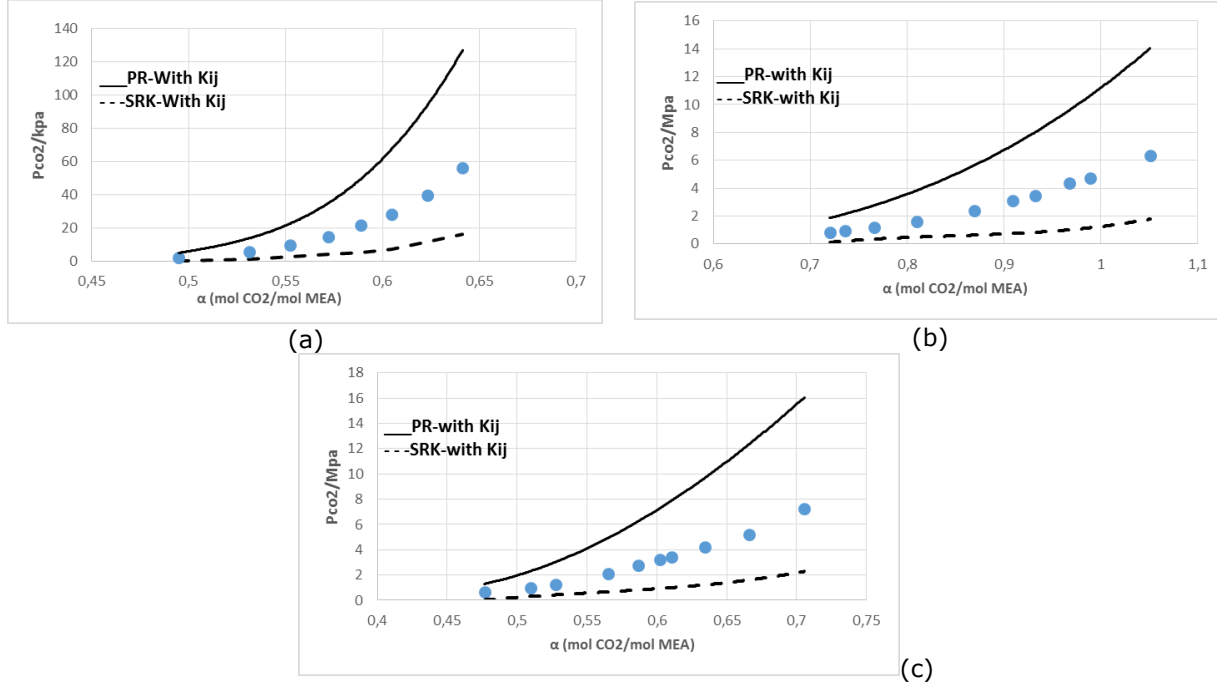


Figure 6. Solubility of  $\text{CO}_2$  in  $\text{CO}_2\text{-H}_2\text{O}\text{-MEA}$  system. a)  $m_{\text{MEA}} = 2.9 \text{ mol} \cdot (\text{kg H}_2\text{O})^{-1}$ ,  $T = 313 \text{ K}$ . b)  $m_{\text{MEA}} = 2.9 \text{ mol} \cdot (\text{kg H}_2\text{O})^{-1}$ ,  $T = 353 \text{ K}$ . c)  $m_{\text{MEA}} = 7.0 \text{ mol} \cdot (\text{kg H}_2\text{O})^{-1}$ ,  $T = 393 \text{ K}$ . ●, Experimental results of Wagner *et al.* [3]; lines: model results considering  $k_{ij}$

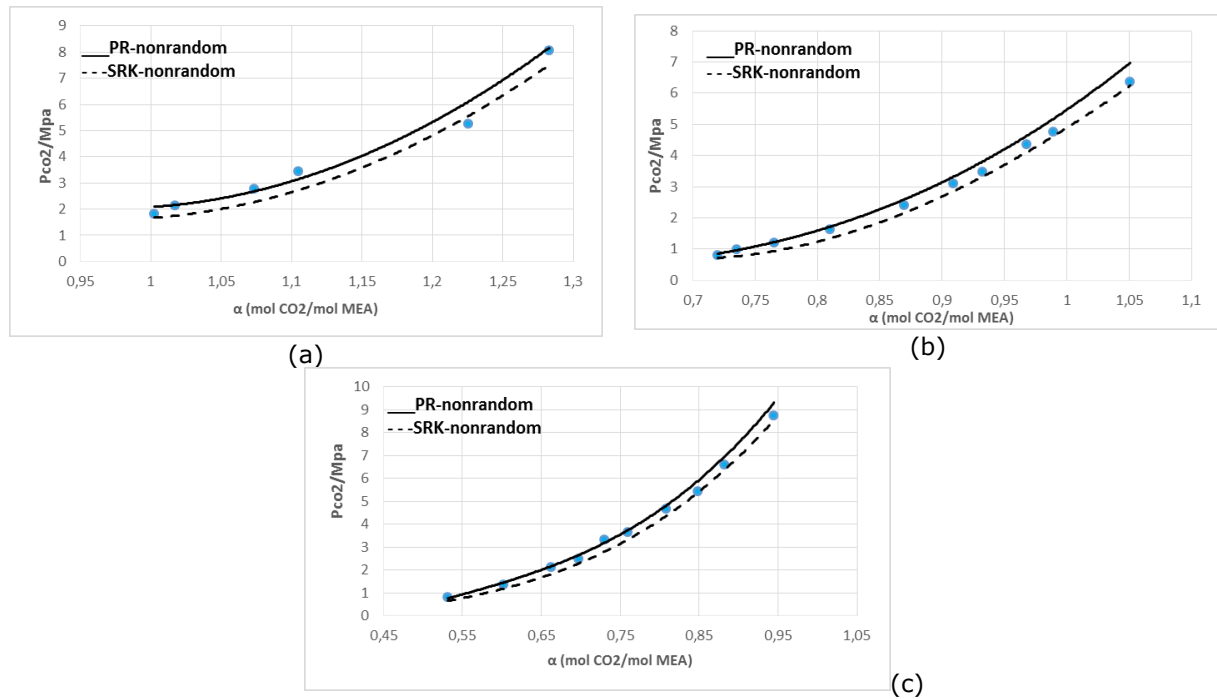


Figure 7. Solubility of  $\text{CO}_2$  in  $\text{CO}_2\text{-H}_2\text{O}\text{-MEA}$  system.  $m_{\text{MEA}} = 2.9 \text{ mol} \cdot (\text{kg H}_2\text{O})^{-1}$ . a)  $T = 313 \text{ K}$ . b)  $T = 353 \text{ K}$ . c)  $T = 393 \text{ K}$ . ●, Experimental results of Wagner *et al.* [3]; lines: model results

Figures 9 and 10 illustrate the solubility of  $\text{CO}_2$  versus its partial pressure in low pressure range (4-80 kPa) for 15 and 30 mass percent of MEA respectively. The AAREs in this case were below 2 percent (1.7) for PR and 3.6 for SRK equations of state. Both of the EOSs have acceptable performance in this pressure range but PR EOS predicts better accurate results

than SRK. The absolute average relative error (AARE) in all cases has been summarized in table 4.

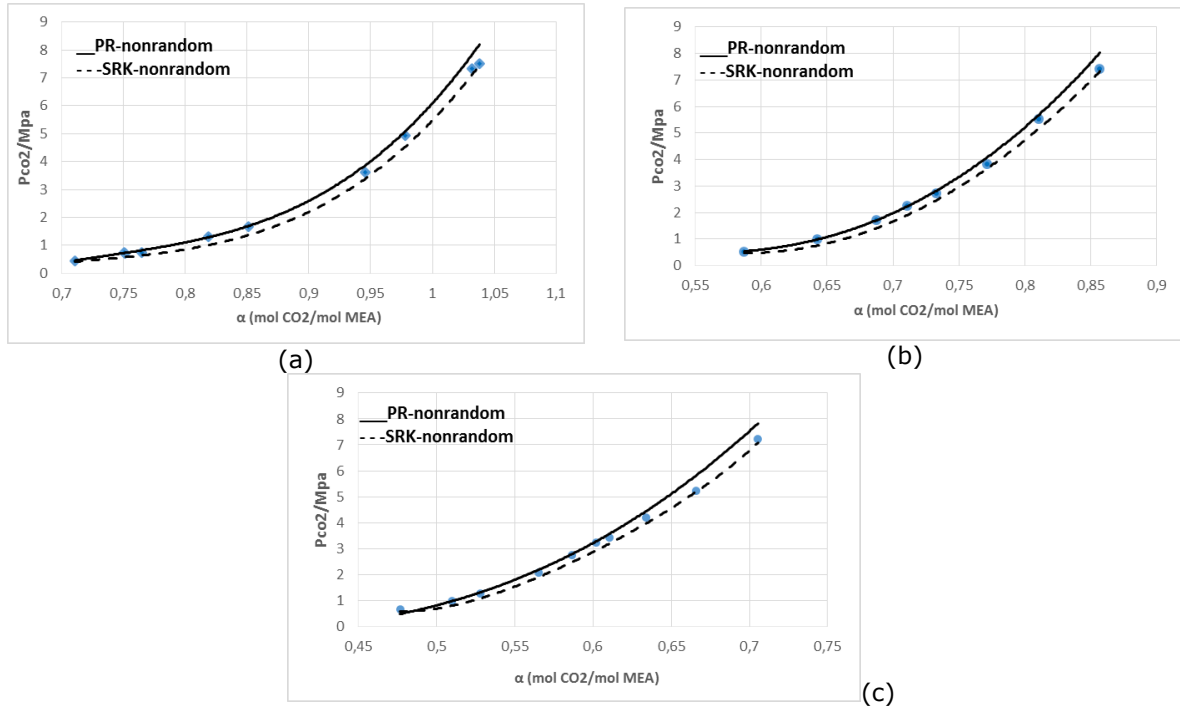


Figure 8. Solubility of  $\text{CO}_2$  in  $\text{CO}_2\text{-H}_2\text{O}\text{-MEA}$  system.  $m_{\text{MEA}} = 7.0 \text{ mol} \cdot (\text{kg H}_2\text{O})^{-1}$ . a)  $T=313 \text{ K}$ . b)  $T=353 \text{ K}$ . c)  $T=393 \text{ K}$ . ●, Experimental results of Wagner et al. [3]; lines: model results

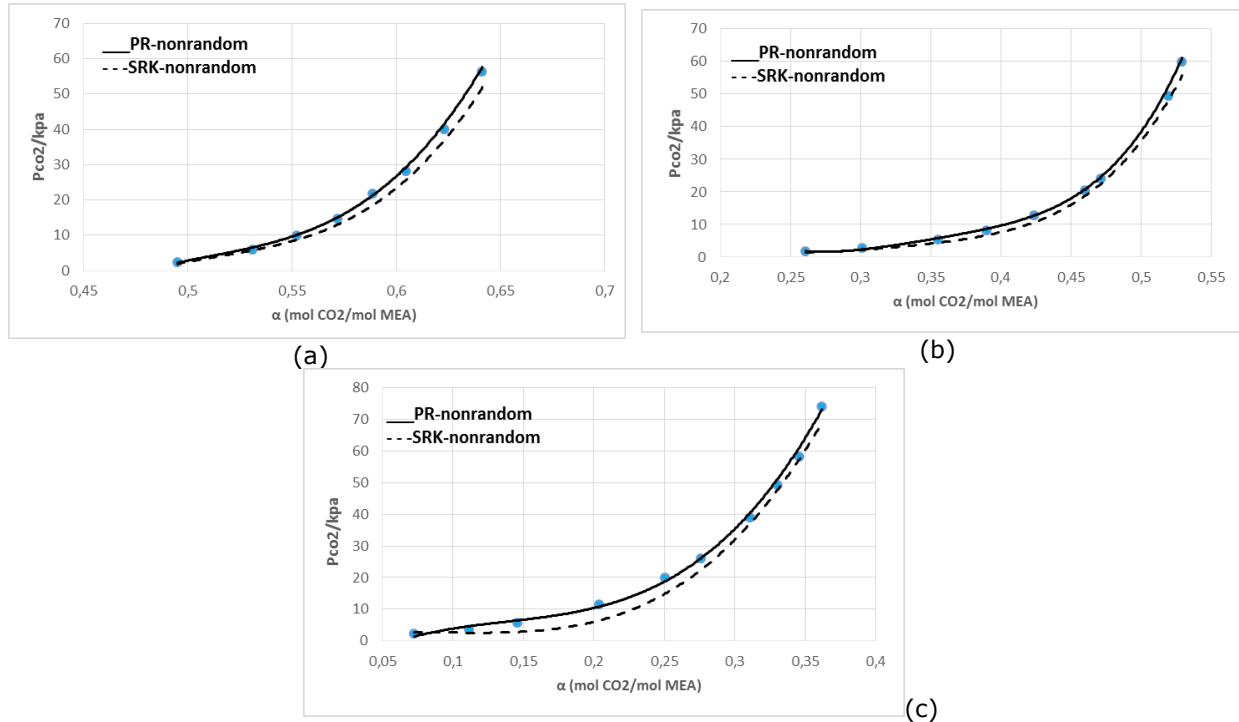


Figure 9. Solubility of  $\text{CO}_2$  in  $\text{CO}_2\text{-H}_2\text{O}\text{-MEA}$  system.  $m_{\text{MEA}} = 2.9 \text{ mol} \cdot (\text{kg H}_2\text{O})^{-1}$ . a)  $T=313 \text{ K}$ . b)  $T=353 \text{ K}$ . c)  $T=393 \text{ K}$ . ●, Experimental results of Wagner et al. [3]; lines: model results

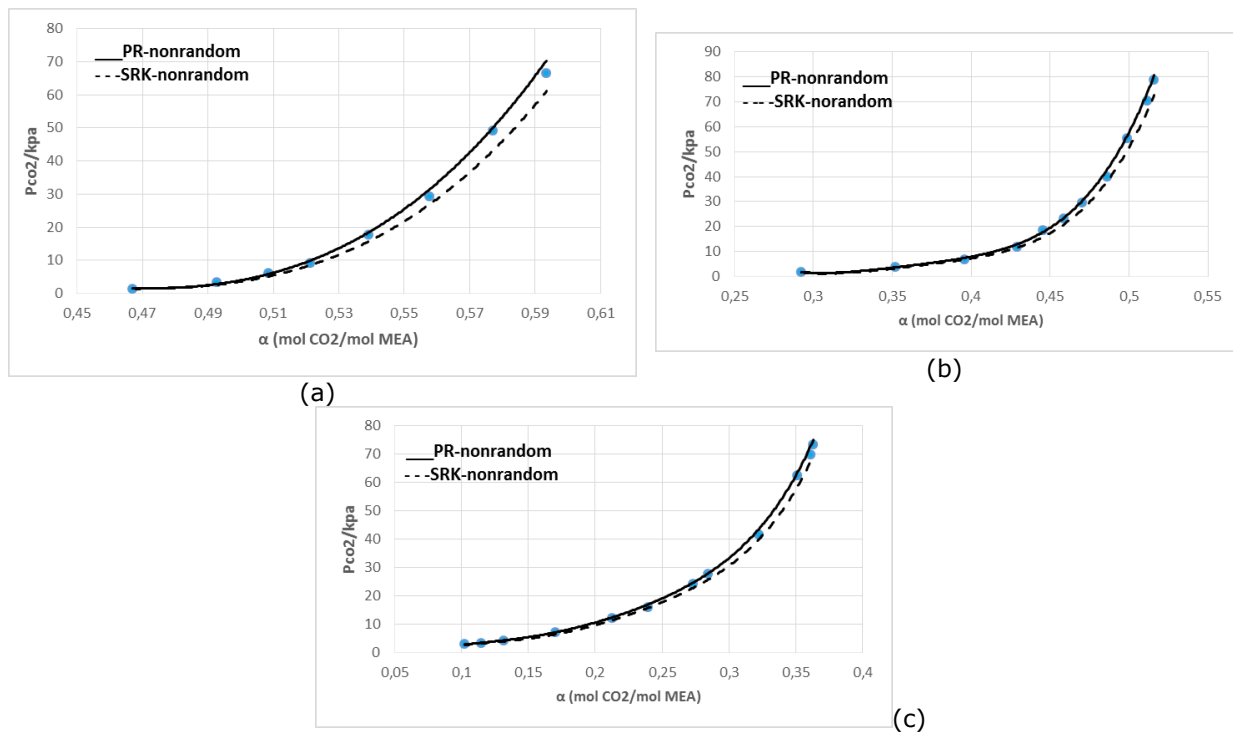


Figure 10. Solubility of  $\text{CO}_2$  in  $\text{CO}_2\text{-H}_2\text{O}\text{-MEA}$  system.  $\bar{m}_{\text{MEA}} = 7.0 \text{ mol} \cdot (\text{kg H}_2\text{O})^{-1}$ . a)  $T=313 \text{ K}$ . b)  $T=353 \text{ K}$ . c)  $T=393 \text{ K}$ . ●, Experimental results of Wagner *et al.* [3]; lines: model results.

### 3.4. Comparison with other models of literature

There are many models in the literature that used to predict the thermodynamic behavior of the  $\text{CO}_2$  solubility in the aqueous solutions of MEA. In order to show the advantageous of this work with respect to other models, we compared our model results to three significant models. These models are Extended UNIQUAC, Quasi-equilibrium and electrolyte NRTL models. In these three models and also in the most of the other existing models in the literature, chemical equilibria were considered besides phase equilibria which makes the modeling more complex and time consuming.

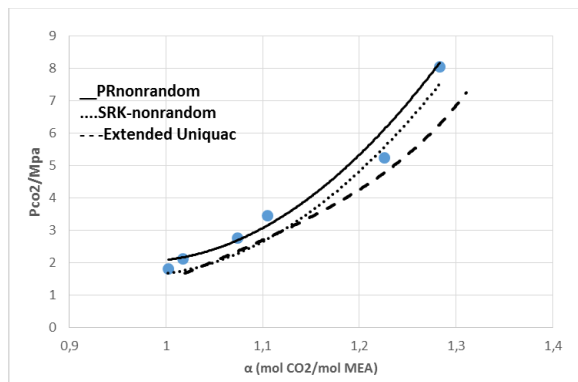


Figure 11. Comparison of the modelling results with the results of extended UNIQUAC model for  $\text{CO}_2\text{-H}_2\text{O}\text{-MEA}$  system. ●, experimental results of Wagner *et al.* [3]. Lines: models result.  $T=313 \text{ K}$ ,  $\bar{m}_{\text{MEA}} = 2.9 \text{ mol} \cdot (\text{kg H}_2\text{O})^{-1}$

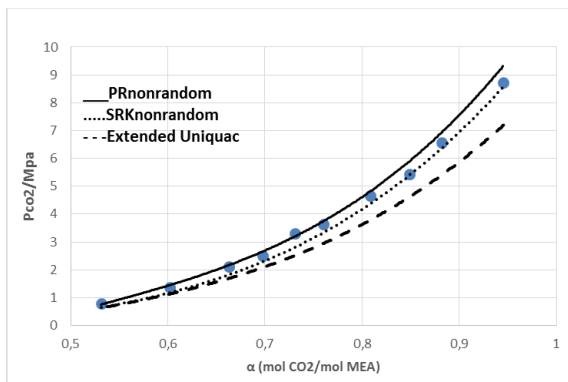


Figure 12. Comparison of the modelling results with the results of extended UNIQUAC model for  $\text{CO}_2\text{-H}_2\text{O}\text{-MEA}$  system. ●, experimental results of Wagner *et al.* [3]. Lines: models result.  $T=393 \text{ K}$ ,  $\bar{m}_{\text{MEA}} = 2.9 \text{ mol} \cdot (\text{kg H}_2\text{O})^{-1}$

Fig. 11 and 12 show the results obtained in this work and the model results of Faramarzi *et al.* [33] which used Extended UNIQUAC model at 313 and 393 K respectively in the high

pressure ranges and  $\bar{m}_{MEA} = 2.9 \frac{mol}{kg \text{ of } H_2O}$  with respect to the experimental data reported by Wagner *et.al.* [3]. As it can be seen from these figures the results of our work are closer to the experimental data. The results of the Extended UNIQUAC model like the results of SRK-nonrandom mixing rules underestimated the partial pressure of the CO<sub>2</sub> in CO<sub>2</sub>-MEA-H<sub>2</sub>O system. Also in the Extended UNIQUAC model, 13 interaction model parameters are needed to be adjusted and 11 of them are temperature-dependent.

A comparison of this work to a quasi-equilibrium model represented by D. Tong *et al.* [57] is shown in figs. 13 and 14. These figures have been sketched for high and low pressure ranges respectively for 313 K and  $\bar{m}_{MEA} = 7.0 \text{ mol} \cdot (\text{kg H}_2\text{O})^{-1}$ . It is clear from these figures that the deviations of this model are also more than present model results of this study especially at the low pressure range. In the quasi-equilibrium model, there were 10 adjustable parameters which three of them were temperature-dependent and seven temperature-independent and the average absolute deviation between this model predictions and their experimental data was within 7%.

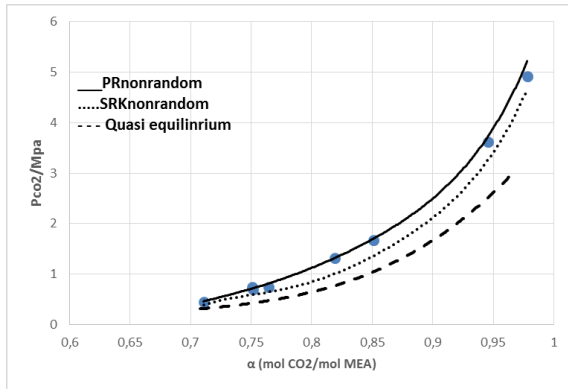


Figure 13. Comparison of the modelling results with the results of a quasi-equilibrium model for CO<sub>2</sub>-H<sub>2</sub>O-MEA system. ●, experimental results of Wagner *et al.* [3]. Lines: models result. T=313K,  $\bar{m}_{MEA} = 7 \text{ mol} \cdot (\text{kg H}_2\text{O})^{-1}$

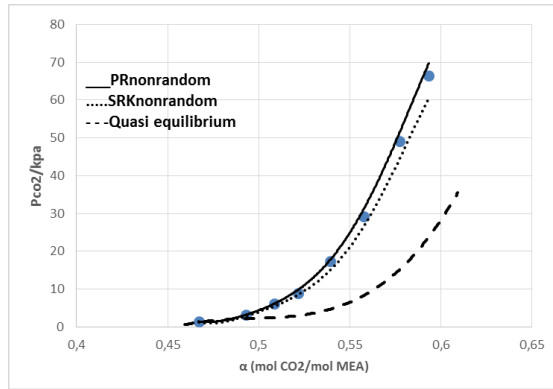


Figure 14. Comparison of the modelling results with the results of a quasi-equilibrium model for CO<sub>2</sub>-H<sub>2</sub>O-MEA system. ●, experimental results of Wagner *et al.* [3]. Lines: models result. T=313K,  $\bar{m}_{MEA} = 7 \text{ mol} \cdot (\text{kg H}_2\text{O})^{-1}$

Figures 15 and 16 compared the results of this work to the results obtained by electrolyte NRTL model which has been done by Y. Zhang *et al.* [58].

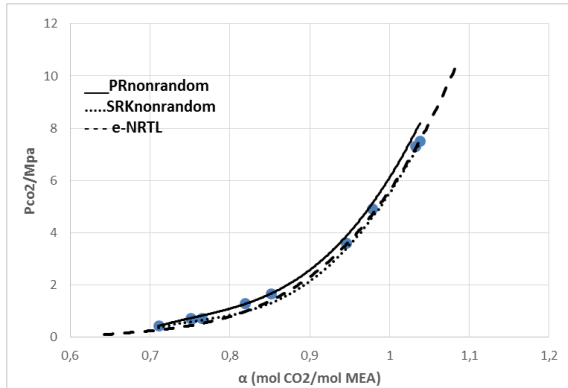


Figure 15. Comparison of the modelling results with the results of e-NRTL model for CO<sub>2</sub>-H<sub>2</sub>O-MEA system. ●, experimental results of Wagner *et al.* [3]. Lines: models result. T=313 K,  $\bar{m}_{MEA} = 7 \text{ mol} \cdot (\text{kg H}_2\text{O})^{-1}$

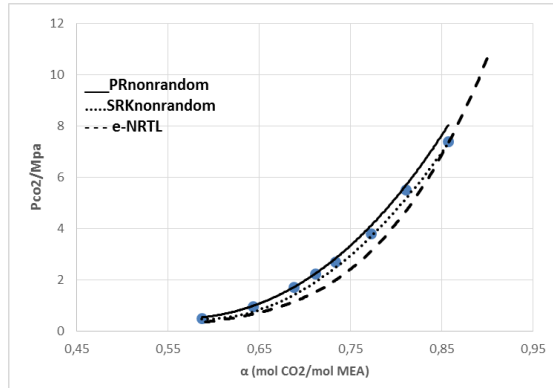


Figure 16. Comparison of the modelling results with the results of e-NRTL model for CO<sub>2</sub>-H<sub>2</sub>O-MEA system. ●, experimental results of Wagner *et al.* [3]. Lines: models result. T=353 K,  $\bar{m}_{MEA} = 7 \text{ mol} \cdot (\text{kg H}_2\text{O})^{-1}$

These figures are sketched for high pressure ranges and in 313 and 353K range respectively with  $m_{MEA} = 7.0 \text{ mol (kg H}_2\text{O)}^{-1}$ . As figures 15 and 16 illustrated the e-NRTL model are in good agreement with the experimental data and the results obtained by Zhang *et al.* study but it needs 12 parameters that should be adjusted with the experimental data. Indeed, the e-NRTL method considered chemical reactions of the system besides phase equilibria which makes the model more rigorous and complicated.

#### 4. Conclusion

In this study the solubility of CO<sub>2</sub> in MEA-H<sub>2</sub>O-CO<sub>2</sub> system has been investigated by PR and SRK equations of state with random and non-random mixing rules. Random mixing rules are not suitable for these aqueous solutions of MEA. Non-Random mixing rules have much better results and sharply reduce the AAREs. For instance, PR EOS had 26.6% errors by random mixing rules while the error reduces to 2.3 % when a non-random mixing rule is used. It is due to the fact that non-random mixing rules consider a term in calculating the attractive forces that is related to polarity and asymmetry of the components. A comparison also has been done between two equation of state (PR and SRK). Both of them have reasonable results in the specific ranges of pressure. PR equation of state works better at low to moderate pressures while the performance of SRK equation of state is better at high pressure range for the examined system. A comparison of the model results to other existing models in the literature such as Extended UNIQUAC, Quasi-equilibrium and e-NRTL models has been done and it was shown that presented model results have less AAREs with respect to Extended UNIQUAC and quasi-equilibrium results. The accuracy of the e-NRTL model is good but it needs many parameters that should be fitted with experimental data and it is also consider chemical reactions of the system which makes the model more complex and rigorous.

#### Nomenclature

Parameter	Dimension	Description
A	-	a parameter for equation of state
a	Pa(m <sup>3</sup> /mol) <sup>2</sup>	a parameter for equation of state
B		a parameter for equation of state
b	m <sup>3</sup> /mol	a parameter for equation of state
f	Pa	fugacity
k <sub>ij</sub>	-	Binary interaction parameter
I <sub>ij</sub>	-	Binary interaction coefficient
m	-	a parameter for equation of state
$\bar{m}$	mol/kg H <sub>2</sub> O	molality
P	Pa	Pressure
P <sub>c</sub>	Pa	Critical pressure
R	j/(mol.K)	Universal gas constant
T	K	Temperature
T <sub>c</sub>	K	Critical temperature
T <sub>r</sub>	-	Reduced temperature
V	m <sup>3</sup> /mol	Molar volume
x <sub>i</sub>	-	Mole fraction in liquid phase
y <sub>i</sub>	-	Mole fraction in vapor phase
Z	-	Compressibility factor

#### Greek letters

$\alpha$	CO <sub>2</sub> loading	$\phi$	fugacity coefficient
$\omega$	acentric factor	$\delta$	constant

#### Abbreviations

PR	Peng-Robinson	MEA	Monoethanolamine
SRK	Soave- Redlich-Kwong	BIP	Binary interaction parameter
EOS	Equation of state		

**References**

- [1] Yamasaki A. An overview of {CO} 2 mitigation options for global warming—emphasizing {CO}2 sequestration options 2003; 36: 361–75.
- [2] Rao AB, Rubin ES. A Technical, Economic, and Environmental Assessment of Amine-Based CO<sub>2</sub> Capture Technology for Power Plant Greenhouse Gas Control. *Environ Sci Technol.*, 2002; 36: 4467–75.
- [3] Wagner M, von Harbou I, Kim J, Ermatchkova I, Maurer G, Hasse H. Solubility of Carbon Dioxide in Aqueous Solutions of Monoethanolamine in the Low and High Gas Loading Regions. *J Chem Eng Data*, 2013; 58: 883–95. DOI:10.1021/je301030z.
- [4] Ye C, Chen G, Yuan Q. Process characteristics of CO<sub>2</sub> absorption by aqueous monoethanolamine in a microchannel reactor. *Chinese J Chem Eng.*, 2012; 20: 111–9. DOI:10.1016/S1004-9541(12)60370-X.
- [5] Cohen SM, Chalmers HL, Webber ME, King CW. Comparing post-combustion CO<sub>2</sub> capture operation at retrofitted coal-fired power plants in the Texas and Great Britain electric grids. *Environ Res Lett.*, 2011; 6: 024001. DOI:10.1088/1748-9326/6/2/024001.
- [6] Tarun CB, Croiset E, Douglas PL, Gupta M, Chowdhury MHM. Techno-economic study of CO<sub>2</sub> capture from natural gas based hydrogen plants. *Int J Greenh Gas Control*, 2007; 1: 55–61. DOI:10.1016/S1750-5836(07)00036-9.
- [7] Rodriguez N, Mussati S, Scenna N. Optimization of post-combustion CO<sub>2</sub> process using DEA-MDEA mixtures. *Chem Eng Res Des.*, 2011; 89: 1763–73. DOI:10.1016/j.cherd.2010.11.009.
- [8] Mofarahi M, Khojasteh Y, Khaledi H, Farahnak A. Design of CO<sub>2</sub> absorption plant for recovery of CO<sub>2</sub> from flue gases of gas turbine. *J. Energy*, 2008; 33: 1311–9. DOI:10.1016/j.energy.2008.02.013.
- [9] Mohammad R.M. Abu-Zahra, Léon H.J. Schneiders, John P.M. Niederer, Paul H.M. Feron GFV. CO<sub>2</sub> capture from power plants. Part I. A parametric study of the technical performance based on monoethanolamine. *Int J Greenh Gas Control*, 2007: 37–46.
- [10] Ali E, Hadj-Kali MK, Mulyono S, Alnashef I, Fakeeha A, Mjalli F, Hayyan A. Solubility of CO<sub>2</sub> in deep eutectic solvents: Experiments and modelling using the Peng–Robinson equation of state. *Chem Eng Res Des.*, 2014; 92: 1898–906. DOI:10.1016/j.cherd.2014.02.004.
- [11] Kohl A& RN. *Gas Purification*. 1997.
- [12] Kidnay JA, Parrish RW. *Fundamentals of Natural Gas Processing*. 2006.
- [13] Ko CC, Chang WH, Li MH. Ternary diffusion coefficients of monoethanolamine and N-methyldiethanolamine in aqueous solutions. *J Chinese Inst Chem Eng*, 2008; 39: 645–51. DOI:10.1016/j.jcice.2008.04.007.
- [14] Qian Z, Guo K. Modelling and Kinetic Study on Absorption of CO<sub>2</sub> by Aqueous Solutions of N-methyldiethanolamine in a Modified Wetted Wall Column. *Chinese J Chem Eng.*, 2009; 17:571–9. DOI:10.1016/S1004-9541(08)60246-3.
- [15] Fouad W a, Berrouk AS. Prediction of H<sub>2</sub>S and CO<sub>2</sub> Solubilities in Aqueous Triethanolamine Solutions Using a Simple Model of Kent–Eisenberg Type. *Ind Eng Chem Res.*, 2012; 51: 6591–7.
- [16] Poormohammadian SJ, Lashanizadegan A, Salooki MK. Modelling VLE data of CO<sub>2</sub> and H<sub>2</sub>S in aqueous solutions of N-methyldiethanolamine based on non-random mixing rules. *Int J Greenh Gas Control*, 2015; 42: 87–97. DOI:10.1016/j.ijggc.2015.07.036.
- [17] Rochelle GT. Amine scrubbing for CO<sub>2</sub> capture. *Science*, 2009; 325: 1652–4. DOI:10.1126/science.1176731.
- [18] Afkhamipour M, Mofarahi M. Sensitivity analysis of the rate-based CO<sub>2</sub> absorber model using amine solutions (MEA, MDEA and AMP) in packed columns. *Int J Greenh Gas Control*, 2014; 25: 9–22. DOI:10.1016/j.ijggc.2014.03.005.
- [19] PV D, McNeil KM. Absorption of carbon dioxide into aqueous amine solutions and effects of catalysis. *Trans Inst Chem Eng Chem Eng.*, 1967; 45: T32.
- [20] Kent R, Eisenberg B. Better data for amine treating. *Hydrocarbon Process*, 1976; 55: 87–90.
- [21] Gabrielsen J, Michelsen ML, Stenby EH, Kontogeorgis GM. A model for estimating CO<sub>2</sub> solubility in aqueous alkanolamines. *Ind Eng Chem Res.*, 2005; 44: 3348–54 DOI:10.1021/ie048857i.
- [22] Rangwala HA, Morrell BR, Mather AE, Otto FD. Absorption of CO<sub>2</sub> into Aqueous Tertiary Amine/MEA Solutions. *Can J Chem Eng.*, 1992; 70: 482–90. DOI:10.1002/cjce.5450700310.

- [23] Deshmukh RD, Mather AE. A mathematical model for equilibrium solubility of hydrogen sulfide and carbon dioxide in aqueous alkanolamine solutions. *Chem Eng Sci.*, 1981; 36: 355–62. DOI:10.1016/0009-2509(81)85015-4.
- [24] Jou F-Y, Mather AE, Otto FD. The solubility of CO<sub>2</sub> in a 30 mass percent monoethanolamine solution. *Can J Chem Eng.*, 1995; 73: 140–7. DOI:10.1002/cjce.5450730116.
- [25] Chen CC, Evans LB. A local composition model for the excess Gibbs energy of aqueous electrolyte systems. *AIChE J.*, 1986; 32: 444–54. DOI:10.1002/aic.690320311.
- [26] Kodýtek V. Thermodynamics of Electrolyte Solutions. *Chem. Listy*, 1999; 93: 170–2. DOI:10.1134/S102833580808003X.
- [27] Austgen DM, Rochelle GT, Chen CC, Peng X. Model of vapor-liquid equilibria for aqueous acid gas-alkanolamine systems using the electrolyte-NRTL equation. *Ind Eng Chem Res.*, 1989; 28: 1060–73. DOI:10.1021/ie00091a028.
- [28] Hessen ET, Haug-Warberg T, Svendsen HF. The refined e-NRTL model applied to CO<sub>2</sub>-H<sub>2</sub>O-alkanolamine systems. *Chem Eng Sci.*, 2010; 65: 3638–48. DOI:10.1016/j.ces.2010.03.010.
- [29] Hilliard MD. A Predictive Thermodynamic Model for an Aqueous Blend of Potassium Carbonate, Piperazine, and Monoethanolamine for Carbon Dioxide Capture from Flue Gas. Dr Thesis Tech Univ Texas Austin 2008:1083.
- [30] le Bouhelec EB, Mougin P, Barreau A, Solimando R. Rigorous modeling of the acid gas heat of absorption in alkanolamine solutions. *Energy and Fuels*, 2007; 21: 2044–55. DOI:10.1021/ef0605706.
- [31] Bishnoi S. Physical and Chemical Solubility of Carbon Dioxide in Aqueous Methyldiethanolamine. 1998.
- [32] Addicks J, Owren GA, Fredheim AO, Tangvik K. Solubility of carbon dioxide and methane in aqueous methyldiethanolamine solutions. *J Chem Eng Data*, 2002; 47: 855–60. DOI:10.1021/je010292z.
- [33] Faramarzi L, Kontogeorgis GM, Thomsen K, Stenby EH. Extended UNIQUAC model for thermodynamic modeling of CO<sub>2</sub> absorption in aqueous alkanolamine solutions. *Fluid Phase Equilib.*, 2009; 282: 121–32. DOI:10.1016/j.fluid.2009.05.002.
- [34] Frst W, Renon H. Representation of excess properties of electrolyte solutions using a new equation of state. *AIChE J.*, 1993; 39: 335.
- [35] Huttenhuis PJG, Agrawal NJ, Hogendoorn JA, Versteeg GF. Gas solubility of H<sub>2</sub>S and CO<sub>2</sub> in aqueous solutions of N-methyldiethanolamine. *J Pet Sci Eng.*, 2007; 55: 122–34. DOI:10.1016/j.petrol.2006.04.018.
- [36] Button J., Gubbins K. SAFT prediction of vapour-liquid equilibria of mixtures containing carbon dioxide and aqueous monoethanolamine or diethanolamine. *Fluid Phase Equilib.*, 1999; 158-160:175–81. DOI:10.1016/S0378-3812(99)00150-8.
- [37] Zoghi AT, Feyzi F, Zarrinpashneh S, Alavi F. Solubility of light reservoir gasses in water by the modified Peng-Robinson plus association equation of state using experimental critical properties for pure water. *J Pet Sci Eng.*, 2011; 78: 109–18. DOI:10.1016/j.petrol.2011.05.001.
- [38] Téllez-Arredondo P, Medeiros M. Modeling CO<sub>2</sub> and H<sub>2</sub>S solubilities in aqueous alkanolamine solutions via an extension of the Cubic-Two-State equation of state. *Fluid Phase Equilib.*, 2013; 344: 45–58. DOI:10.1016/j.fluid.2013.01.005.
- [39] Danesh A. PVT and phase behaviour of petroleum reservoir fluids. vol. 47. 1998.
- [40] Peng D-Y, Robinson DB. A New Two-Constant Equation of State. *Ind Eng Chem Fundam.*, 1976; 15: 59–64. DOI:10.1021/i160057a011.
- [41] Soave G. Equilibrium constants from a modified Redlich-Kwong equation of state. *Chem Eng Sc.*, 1972; 27: 1197–203. DOI:10.1016/0009-2509(72)80096-4.
- [42] Rowlinson J. Molecular thermodynamics of fluid-phase equilibria. *J Chem Thermodyn.*, 1970; 2: 158–9. DOI:10.1016/0021-9614(70)90078-9.
- [43] Mathias PM, Naheiri T, Oh EM. A density correction for the Peng-Robinson equation of state. *Fluid Phase Equilib.*, 1989; 47: 77–87. DOI:10.1016/0378-3812(89)80051-2.
- [44] Voros NG, Tassios DP. Vapor-liquid equilibria in nonpolar/weakly polar systems with different types of mixing rules. *Fluid Phase Equilib.*, 1993; 91: 1–29. DOI:10.1016/0378-3812(93): 85076-X.
- [45] Bjorlykke OP, Firoozabadi A. Measurement and Computation of Near-Critical Phase Behavior of a C<sub>1</sub>/nC<sub>24</sub> Binary Mixture. *SPE Reserv Eng.*, 1992; May: 271–7.

- [46] Danesh A, Xu DH, Todd AC. Comparative study of cubic equations of state for predicting phase behaviour and volumetric properties of injection gas-reservoir oil systems. *Fluid Phase Equilib.*, 1991; 63: 259–78. DOI:10.1016/0378-3812(91)80036-U.
- [47] Nasrifar K, Bolland O. Prediction of thermodynamic properties of natural gas mixtures using 10 equations of state including a new cubic two-constant equation of state. *J Pet Sci Eng.*, 2006; 51: 253–66. DOI:10.1016/j.petrol.2006.01.004.
- [48] Knudsen K, Stenby EH, Fredenslund AA. A comprehensive comparison of mixing rules for calculation of phase equilibria in complex systems. *Fluid Phase Equilib.*, 1993; 82: 361–8.
- [49] Avlonitis D, Danesh A, Todd AC. Prediction of VL and VLL equilibria of mixtures containing petroleum reservoir fluids and methanol with a cubic EoS. *Fluid Phase Equilib.*, 1994; 94: 181–216. DOI:10.1016/0378-3812(94)87057-8.
- [50] Mathias PM, Klotz HC, Prausnitz JM. Equation-of-State mixing rules for multicomponent mixtures: the problem of invariance. *Fluid Phase Equilib.*, 1991; 67:31–44. DOI:10.1016/0378-3812(91)90045-9.
- [51] Masoudi R, Tohidi B. On modelling gas hydrate inhibition by salts and organic inhibitors. *J Pet Sci Eng.*, 2010; 74: 132–7. DOI:10.1016/j.petrol.2010.08.010.
- [52] NASRI Z. Applications of the Peng-Robinson Equation of State using MATLAB. vol. 43. 2009.
- [53] Lee JI, Otto FD, Mather AE. Equilibrium between carbon dioxide and aqueous monoethanolamine solutions. *J Appl Chem Biotechnol.*, 1976; 26:541–9. DOI:10.1002/jctb.5020260177.
- [54] Lee JI, Otto FD, Mather AE. The solubility of H<sub>2</sub>S and CO<sub>2</sub> in aqueous monoethanolamine solutions. *Can J Chem Eng.*, 1974; 52:803–5. DOI:10.1002/cjce.5450520617.
- [55] Shen KP, Li MH. Solubility of carbon dioxide in aqueous mixtures of monoethanolamine with methylidiethanolamine. *J Chem Eng Data* 1992; 37: 96–100.
- [56] Ma'mun S, Nilsen R, Svendsen HF, Juliussen O. Solubility of carbon dioxide in 30 mass % monoethanolamine and 50 mass % methylidiethanolamine solutions. *J Chem Eng Data*, 2005; 50: 630–4. DOI:10.1021/je0496490.
- [57] Tong D, Trusler JPM, Maitland GC, Gibbins J, Fennell PS. Solubility of carbon dioxide in aqueous solution of monoethanolamine or 2-amino-2-methyl-1-propanol: Experimental measurements and modelling. *Int J Greenh Gas Control*, 2012; 6:37–47. DOI:10.1016/j.ijggc.2011.11.005.
- [58] Zhang Y, Que H, Chen CC. Thermodynamic modeling for CO<sub>2</sub> absorption in aqueous MEA solution with electrolyte NRTL model. *Fluid Phase Equilib.*, 2011; 311:67–75. DOI:10.1016/j.fluid.2011.08.025.

*To whom correspondence should be addressed. M. Koolivand Salooki, Gas Research Division, Research Institute of Petroleum Industries, Tehran 14665-1998, Iran, [mehdi.koolivand@ut.ac.ir](mailto:mehdi.koolivand@ut.ac.ir)*